Parameter Estimation for Reactive Transport by a Monte-Carlo Approach

Mohit Aggarwal and Jérôme Carrayrou
Institut de Mécanique des Fluides et des Solides de l'Université Louis Pasteur, UMR 7507 Université Louis Pasteur-CNRS, 2 rue Boussingault, 67000 Strasbourg, France

DOI 10.1002/aic.10813
Published online April 17, 2006 in Wiley InterScience (www.interscience.wiley.com).

The chemical parameters used in reactive transport models are not known accurately due to the complexity and the heterogeneous conditions of a real domain. The development of an efficient algorithm in order to estimate the chemical parameters using Monte-Carlo method is presented. By fitting the results obtained from the model with the experimental curves obtained with various experimental conditions, the problem of parameters estimation is converted into a minimization problem. Monte-Carlo methods are very robust for the optimization of the highly nonlinear mathematical model describing reactive transport. It involves generating random values of parameters and finding the best set. The focus is to develop an optimization algorithm which uses less number of realizations so as to reduce the CPU time. Reactive transport of TBT through natural quartz sand at seven different pHs is taken as the test case. Our algorithm will be used to estimate the chemical parameters of the sorption of TBT onto the natural quartz sand. © 2006 American Institute of Chemical Engineers *AIChE J,* 52: 2281–2289, 2006
Keywords: reactive transport, numerical modeling, Monte-Carlo simulation, parameters estimation

Introduction

Recent developments in reactive transport modeling makes reactive transport models more and more used for simulating, describing, improving comprehension, or providing prevision[1] for hydrogeologists or geochemists. They are used in highly sensitive domains, such as ground water supply preservation, development of pollution remediation scenarii or nuclear waste storage study. Geochemical systems described by these numerical models become more and more complex, mainly by an increase of the chemical phenomenon complexity. A reactive transport model needs five kinds of inputs: the hydraulic properties of the domain, the chemical reactions occurring and the chemical parameters, the boundary and initial conditions. We will focus here on the chemical part of the problem. To describe a reactive transport model, a set of chemical reactions is first chosen and after that the corresponding parameters are obtained, whatever the way. Nevertheless, the required chemical parameters are not known exactly. Because the described phenomena are nonlinear, low precision on the determination of the parameters can lead to rejection of an accurate set of reactions. Moreover, it is impossible to determine if the divergence between the experimental results, and the calculated one is due to a false set of reactions or insufficiently precise determination of the parameters. Today, parameters estimation is mainly done using batch experiments with unique experimental conditions with tools like FITEQL.[2] Estimated parameters are then accurate for batch reactor and for a given experimental state, such as imposed pH or fixed ionic force. Extrapolating these parameters to natural uncontrolled systems is then very hazardous. The aim of this work is to present a way to estimate parameters for most realistic cases by a Monte-Carlo procedure. The reactive transport parameters will be estimated from column experiments. Calculated elution curves of an injection-leaching experiment will be fitted to experimental elution curves. In order to lead to parameters that will not (or less) depend on the experimental conditions; many elution curves obtained at different pH will be simultaneously fitted.

Because of the high nonlinearity of the mathematical model

Correspondence concerning this article should be addressed to J. Carrayrou at carrayro@imfs.u-strasbg.fr
Mohit Aggarwal is also affiliated with Indian Institute of Technology, Dept. of Chemical Engineering, New Dehli, India

describing reactive transport under instantaneous equilibrium assumption, we prefer a Monte-Carlo method instead of a gradient-like one. Indeed, it is well known that gradient-like methods are very efficient if there is a linear relation between the parameters and the objective function. Nonlinear equations are then always associated to difficulties on performing inverse modeling as explain by Zhang and Guay.[3] For nonlinear relations, such as equilibrium chemical equations, their efficiency decreases strongly. It has been well established[4,5] that gradient methods are sometime unable to solve some batch equilibrium problems. For batch equilibrium, nonconvergence of gradient method is due to local minima, flat zone of the error function or infinite loop phenomena.[5] Extrapolation of these conclusions to inverse modelling of reactive transport lets expect many convergence problems for gradient like methods as assumed by Marshall.[6] Even if the Monte-Carlo methods are more time-consuming, they are indeed more robust than the gradient-like methods because they do not use the slope of the objective function. A Monte-Carlo method has been successfully used for sensitivity analysis of coagulation processes.[7] Moreover, these authors used a Monte-Carlo approach to obtain the derivative of the objective function before running a gradient-like method for the parameters estimation.

We first present the numerical model: the advection-dispersion-reaction (ADR) equation is detailed, and we present the methods used to solve it as fast as possible. After that, we explain the methods used for parameter estimations: the Monte-Carlo procedure, the error function and the optimization procedures.

A results section is devoted to the study of the developed algorithm. A column experiment on sorption of tributyltin onto a natural quartz sand[8,9] at seven different pH is used as test case. We show the efficiency of the algorithm developed. We then discuss the results obtained through our optimization procedure, and we compare them to results obtained from batch calculation at one pH.

Numerical Model

Reactive transport equation

Under the assumptions of instantaneous equilibrium and identical dispersion of solutes, the ADR equation can be written like Eq. 1 for the Nx component j of the system

$$\omega \frac{\partial (Td_j + Tf_j)}{\partial t} = \nabla \cdot [\mathbf{D} \cdot \nabla (Td_j)] - U \cdot \nabla (Td_j) \quad \text{for } j = 1 \text{ to } Nx \quad (1)$$

where, ω $(-)$ is the active porosity, $\mathbf{D}$ (m^2/s) the dispersion tensor, U (m/s) the Darcy velocity, Td_j (mol/dm^3) the total mobile concentration of component j and Tf_j (mol/dm^3) the total nonmobile concentration of component j. The chemical system is described by mass action and conservation laws. The mass action laws Eq. 2 are written for the formation of the Nc species C_i by the selected component set X_j

$$\{C_i\} = K_i \cdot \prod_{j=1}^{Nx} \{X_j\}^{a_{i,j}} \quad \text{for } i = 1 \text{ to } Nc \quad (2)$$

where the activity of species and component is noted $\{-\}$, K_i is the equilibrium constant, Nx the number of components used to describe the system, and $a_{i,j}$ the stochiometric coefficient for the mass action law. For precipitated minerals, the mass action laws are written under the precipitation product form Eq. 3 if precipitation occurs

$$1 = Kp_i \cdot \prod_{j=1}^{Nx} \{X_j\}^{ap_{i,j}} \quad (3)$$

Kp_i is the precipitation product of precipitated species Cp_i and $ap_{i,j}$ are the stochiometric coefficients. The conservation law Eq. 4 is written to conserve the total quantity $[T_j]$ (mol/dm^3) of each component

$$[T_j] = \sum_{i=1}^{Nc} b_{i,j} \cdot [C_i] + \sum_{i=1}^{NcP} bp_{i,j} \cdot [Cp_i] \text{ for } j = 1 \text{ to } Nx \quad (4)$$

where the concentrations (mol/dm^3) are noted $[-]$, Nc (resp., NcP) is the number of species (resp., precipitated) in the system, and $b_{i,j}$ (resp., $bp_{i,j}$) the stochiometric coefficient of species C_i (resp. Cp_i) for the conservation law. Stochiometric coefficients used for the mass-action law are different than those used for the conservation law in the model SPECY.[10] This allows the description of some geochemical processes, such as surface precipitation.[11]

Substituting the species activity from Eq. 2 instead of the species concentration into the conservation law Eq. 4 is done by using activity coefficient γ_i and leads to the nonlinear algebraic system Eq. 5.

$$[T_j] = \sum_{i=1}^{Nc} b_{i,j} \cdot \frac{K_i}{\gamma_i} \prod_{k=1}^{Nx} (\gamma_k [X_k])^{a_{i,k}} + \sum_{i=1}^{NcP} b_{i,j} \cdot [Cp_i] \quad \text{for } j = 1 \text{ to } Nx$$

$$1 = Kp_i \cdot \prod_{j=1}^{Nx} \{X_j\}^{ap_{i,j}} \text{ for } i = 1 \text{ to } NcP \quad (5)$$

The system Eq. 5 is of size $Nx + NcP$, and the unknowns are the component $[X_j]$, and the precipitated species $[Cp_i]$ concentrations (mol/dm^3). Activity coefficient are calculated using the Davies model,[11,12,13] which is accurate for ionic strength $I < 0.5$

$$\log(\gamma_i) = -A \cdot z_i^2 \cdot \left(\frac{\sqrt{I}}{1 + \sqrt{I}} - B \cdot I \right) \quad (6)$$

where $A = 1.82 \cdot 10^6 \cdot (\varepsilon \cdot T)^{-3/2}$, T is the Kelvin temperature, ε the electric permeability of water and $B = 0.24$.

The mobile total concentration Td_j, and the nonmobile total concentration Tf_j of component j are calculated from the sum of the concentration of the NcD mobile species, and NcF non-mobile species

$$[Td_j] = \sum_{i=1}^{NcD} b_{i,j} \cdot [C_i] \text{ and } [Tf_j] = \sum_{i=1}^{NcF} b_{i,j} \cdot [C_i] + \sum_{i=1}^{NcP} b_{i,j} \cdot [Cp_i] \quad \text{for } j = 1 \text{ to } Nx \quad (7)$$

Because the solution of Eq. 5 is unique for a given set of T_j, the combination of Eq. 5 and Eq. 7 can be noted Eq. 8

$$[Td_j] = fd_j([T_j]) \text{ and } [Tf_j] = ff_j([T_j]) \text{ for } j = 1 \text{ to } Nx \quad (8)$$

where the total concentration T_j is the sum of the mobile Td_j, and nonmobile Tf_j total concentration for each component.

Sorption phenomena can be described easily by ion exchange or by surface complexation. For ion exchange, the mass action law describing the formation of a species is given in Eq. 2. For surface complexation phenomenon, the sorption site should be defined as a component X_s. Then the potential of the surface Ψ is added to the mass action law describing the sorption of a species Cs_i

$$\{Cs_i\} = K_i \cdot \exp\left(-\frac{z_i F}{R\tau} \cdot \Psi\right) \cdot \prod_{j=1}^{Nx} \{X_j\}^{a_{i,j}} \quad (9)$$

where z_i is the charge of the species Cs_i, R is the gas constant, F is the Faraday constant, and τ is the temperature.

Different models can be used to obtain the potential Ψ from the electrostatic charge fixed at the surface.[11,14,15] In this work, only the diffuse layer model (DLM) will be used

$$\sum_{sorbed} z_i \cdot [Cs_i] = \frac{S \cdot M}{F} (8 \cdot R \cdot \tau \cdot \varepsilon \cdot \varepsilon_0 \cdot I)^{1/2} \cdot \sinh\left(\frac{Z_{el} \cdot F \cdot \Psi}{2 \cdot R \cdot \tau}\right) \quad (10)$$

where ε_0 is the permittivity of vacuum, ε the permittivity of water, Z_{el} the electrical charge of counterion, S the specific area of the solid, and M the mass concentration of the solid. By defining the electrostatic potential as a component X_Ψ and the associated stochiometric coefficient $a_{i,\Psi}$

$$\{X_\Psi\} = \exp\left(-\frac{F}{R\tau} \cdot \Psi\right) \text{ and } a_{i,\Psi} = z_i \quad (11)$$

We can include the complexation surface phenomena into the general formulation presented by Eqs. 2 and 4. The mass action law Eq. 9 is also written

$$\{Cs_i\} = K_i \cdot \{X_\Psi\}^{a_{i,\Psi}} \cdot \prod_{j=1}^{Nx} \{X_j\}^{a_{i,j}} \quad (12)$$

and the conservation law Eq. 4 is expressed as Eq. 13 with the DLM model Eq. 10.

$$T_\Psi = \frac{S \cdot M}{2F} \cdot \sqrt{8 \cdot R\tau \cdot \varepsilon \cdot \varepsilon_0 \cdot I} \cdot (\{X_\Psi\}^{-(Z_{el}/2)} - \{X_\Psi\}^{Z_{el}/2}) = \sum_{sorbed} a_{i,\Psi} \cdot [Cs_i] \quad (13)$$

Reactive transport model

In order to reduce to minimum the computation time, efficient numerical methods are used. The computer code SPECY solves the advection-dispersion-reaction Eq. 1 by an operator-splitting scheme. As shown by several authors[10,16,17] the best way to solve ADR equation under instantaneous equilibrium assumption by OS is to use a standard iterative scheme.[18]

The resolution procedure is described by Eqs. 14 and 15

$$\omega \frac{Td_j^{n+1,k+1} - Td_j^n}{\Delta t} = \nabla \cdot [\mathbf{D} \cdot \nabla(Td_j)] - U \cdot \nabla(Td_j) - \omega \frac{Tf_j^{n+1,k} - Tf_j^n}{\Delta t} \text{ for } j = 1 \text{ to } Nx \quad (14)$$

$$[Tf_j^{n+1,k+1}] = ff_j([Td_j^{n+1,k+1}] + [Tf_j^{n+1,k}]) \text{ for } j = 1 \text{ to } Nx, \text{ with } [Tf_j^{n+1,0}] = [Tf_j^n] \quad (15)$$

The advective part of the equation is solved by the discontinuous finite element method and the dispersive part by the mixed hybrid finite element method. The combination of this resolution method and a standard iterative OS scheme leads to a very accurate solution, even if the mesh size is large.[18] It is well known that the maximum computing time is spent for the geochemical computation and not for the transport one. To reduce geochemical computation, SPECY solves the nonlinear algebraic system Eq. 5 with an efficient algorithm.[5] The positive continuous fraction method is used as a preconditioner to obtain an intermediate solution, close to the exact one. Then the Newton-Raphson method is used to obtain the final solution. To increase the efficiency of the Newton-Raphson method, SPECY limits the research procedure to the chemically allowed interval. This specific algorithm reduces the computing time of geochemical computation.

All these implementations lead to faster computing of reactive transport phenomena. These implementations are useful because the number of realizations needed by a Monte-Carlo approach is very high.

Monte-Carlo procedure

In order to reduce the computing time, the number of parameters N_P which will be estimated is reduced to a minimum. Hydrodynamic parameters, such as porosity, velocity or dispersivity are estimated from tracer experiment, and are assumed to be well known. By the same way, chemical parameters for aqueous reactions, such as equilibrium constants and concentrations are obtained from thermodynamic databases, and are assumed to be well known. Only chemical parameters related to the solid-water interface phenomena are estimated, that is, equilibrium constant for sorption reactions, total concentration for sorption components and surface complexation parameter, such as specific area or capacitance.

Parameters **P** which have to be estimated are randomly generated. The distribution of each parameter P_i describes a Gaussian distribution. Each Gaussian distribution is set by its mean $\bar{P}_i$ and its standard deviation σ_i. There are two ways of sampling random numbers from a given set of probability distribution:

(1) Monte Carlo (MC): In this method we generate a random probability value between the given range and map it onto the corresponding parameter value. To generate more parameter values, we just repeat the procedure independently. Using this method, we need large sets of parameter values to have a distribution close to the actual one.

(2) Latin Hyper Cube (LHC): In LHC we divide the given range of parameter values into regions of equal probability. A random value of parameter is then generated in each interval. This method ensures that we cover the whole range of parameter values, and it gives distribution close to the actual one even if the number of generated random values is limited.

It is clear that the LHC method is more accurate and efficient.[19] Thus, we will be using LHC method to generate random numbers.

Objective function

In order to compare the generated set of parameter **P** and to find the best one, the following objective function F_D is used

$$F_N(\mathbf{P}) = \frac{1}{N_{Exp}} \sum_{Experiment} \left(\frac{\theta_{Exp}}{N_{Mes}} \cdot \sum_{Mesure} \theta_{Mes} \sqrt{\left[\frac{C_{Mes} - C_{Calc}(\mathbf{P})}{C_{Mes} + \varepsilon} \right]^2} \right) \tag{16}$$

where N_{Exp} is the number of different experiments to fit, θ_{Exp} is the weight of each experiment. N_{Mes} is the number of experimental points for each experiment, θ_{Mes} is the weight of each experimental point, C_{Mes} is the measured concentration, and C_{Calc} is the calculated concentration. The weight of each experiment θ_{Exp} and of each experimental point θ_{Mes} are defined by the modeller in order to give more or less importance to an experiment or to a point. These values are generally defined depending on the measured error. The limiting parameter ε is used to reduce the influence of very small concentration in the construction of the objective function. Practically, we set ε equal to the detection limit of measurement procedure used during the experiments. We use $\frac{C_{Mes} - C_{Calc}}{C_{Mes} + \varepsilon}$ in the objective function in order to give the same importance to small concentrations than to higher one.

Optimization procedure

The objective of the optimization procedure is to find the best set of parameters. It is well known that Monte-Carlo procedures are time consuming. In order to reduce CPU time, we combine an automatic procedure to find a minimum of the objective function and an expert analysis to determine if the given minimum is a local or a global one. We have tested other procedures, such as simulated annealing but these kinds of methods are too much time consuming in our case. Because the computing time of one realization is quite long, it is more efficient to analyze manually the validity of the proposed set of parameters.

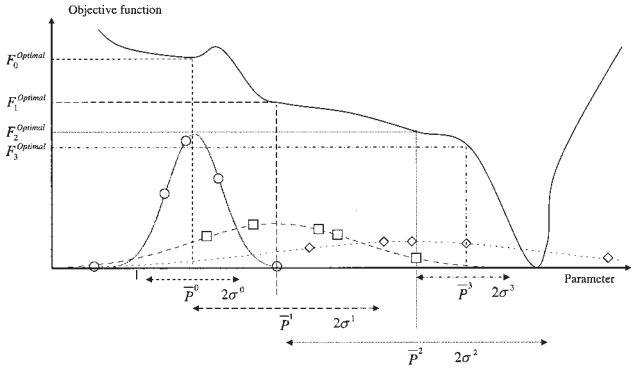

Figure 1. Optimization procedure for a single parameter problem.

We plot the Gaussian curves used for the parameter generator and $N_I = 5$ parameter values for three optimization steps.

Automatic optimization. To reduce the CPU time, we change the mean $\bar{\mathbf{P}}$ and the standard deviation $\boldsymbol{\sigma}$ of the Gaussian curves used to generate the parameters **P** during the optimization procedure.

We first generate $N_I = 100$ sets of parameters $\mathbf{P}^k$ from $\bar{\mathbf{P}}^i$ and $\boldsymbol{\sigma}^i$ (see Figure 1). Initial mean $\bar{\mathbf{P}}^0$ and standard deviation $\boldsymbol{\sigma}^0$ are given by the modeler. The first minimal value of the objective function is $F^{Min} = F(\bar{\mathbf{P}}^0)$. The reactive transport problem is solved with these sets of parameters, and the objective function $F^k(\mathbf{P}^k)$ is then calculated for $k = 1$ to N_I. We then compare the N_I objective functions and select the smallest $F^{Optimal}$. If $F^{Optimal} < F^{Min}$ then we change the mean by taking $\bar{\mathbf{P}}^{i+1} = \mathbf{P}^{Optimal}$, the standard deviation by taking

$$\boldsymbol{\sigma}^{i+1} = \mathrm{Max}[|\mathbf{P}^{Optimal} - \bar{\mathbf{P}}^i|; (\alpha_\sigma \cdot \boldsymbol{\sigma}^i)]. \tag{17}$$

and the value of F^{Min} by taking $F^{Min} = F^{Optimal}$ as shown in Figure 1.

We use Eq. 17 to adapt the standard deviation. α_σ is a parameter which have to limit the reduction of the standard deviation. The optimal set of parameters $\mathbf{P}^{Optimal}$ is sometimes very close to the previous one $\bar{\mathbf{P}}^i$. This can lead to a very fast reduction of the standard deviation and, consequently, a severe reduction of the convergence speed of the algorithm. In this work, we use $\alpha_\sigma = 0.5$ as shown in Figure 2. This ensures a sufficiently slow reduction of the standard deviation and a good convergence speed.

If $F^{Optimal} > F^{Min}$, we reject the proposed set of parameters and increase the value of N_I by taking $N_I = 1{,}000$. Then we run again N_I realizations with the same mean $\mathbf{P}^i$ and $\boldsymbol{\sigma}^i$. In this case, we change the mean and the standard deviation immediately when a better set is found. After that, if no minimum is found, the standard deviation is decreased and $\boldsymbol{\sigma}^{i+1} = \boldsymbol{\sigma}^i/2$. We have tested to increase the standard deviation. However, this choice requires more realizations to cover all the ranges of the parameter values with a sufficiently small interval, and is very CPU time consuming. It seems that the minimum of the error function is a very small hole in a quite flat area, as for batch equilibrium calculation.

We choose $N_I = 100$ at the beginning of the algorithm

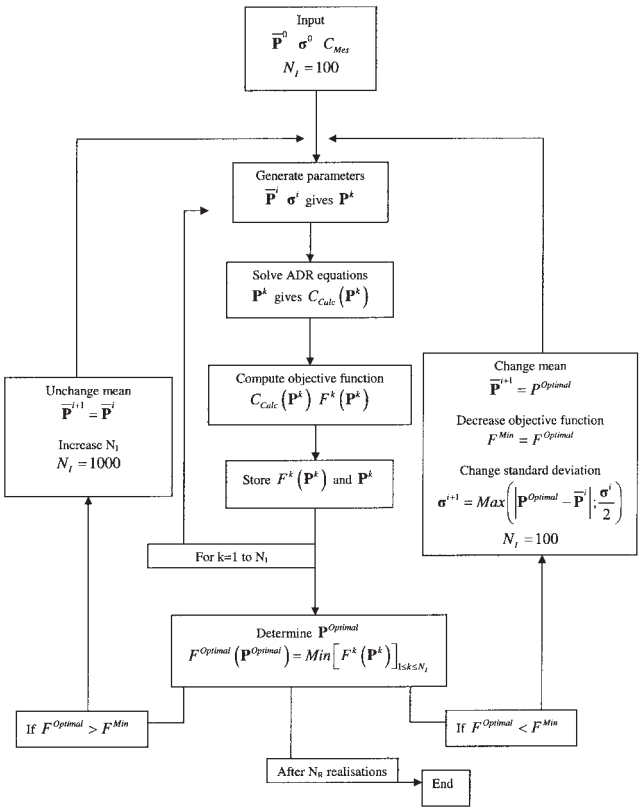

Figure 2. Optimization algorithm.

because this number of realizations is enough to give a good representation of a Gaussian curve for each parameter using the LHC sampling method. Decreasing the value of N_I reduces the robustness of the algorithm, but it increases the convergence rate. Convergence becomes then less and less probable. Increasing the value of N_I increases the robustness of the algorithm, making convergence to the accurate solution more and more certain, but increases the computing time too.

This cycle (running N_I realization, selecting the best set, changing the mean and the standard deviation) is usually done 20 times. The total number of realizations is then $N_R = 2{,}000$. The best set of parameters and the associated standard deviation have to be analyzed to determine their validity.

Expert analysis

The total number of realization used here ($N_R = 2{,}000$) is not large enough to ensure the convergence to the global minima. Some numerical methods can be used to increase the probability of convergence: increasing N_R; performing simulated annealing. Unfortunately, these methods are too time consuming in our case. In order to reduce the time needed to find the minimum, we use the following procedure:

(a) Running three to six automatic optimizations using the initial guess of parameters.

(b) Selecting one to three acceptable sets of parameters.

(c) Running one to three automatic optimizations using each selected set of parameters. The initial standard deviations can be smaller than those used at the stage (a).

(d) Repeating stages (b) and (c) until there is only one set of parameters left. The initial standard deviations can be reduced. This set of parameters cannot be improved by an automatic optimization.

(e) Analyzing the correlations between the fitted parameters.

This procedure ensures that the fitted set of parameters correspond to a minimum of the objective function.

The selection of the acceptable sets of parameters (stage b) uses the objective functions and some additional informations. The sets associated to the higher objective functions are rejected. It is useful to have some additional informations which are not injected into the optimization procedures. These informations can be estimated values of some parameters, or a relation between some parameters. They can be obtained by another experiment than those used to perform the optimization.

Results and Discussion

Reactive transport test-case

The reactive transport test-case we use has been given by Bueno et al.[8,9] It is about transport of TBT through a natural quartz sand. These authors provide breakthrough curves of TBT at seven different pH.[8] This leads to seven different sets of Langmuir parameters. From Langmuir parameters obtained by these authors at pH = 6.1, equilibrium constants and site concentration for the sorption of TBT onto the natural quartz sand can be calculated. Specific area of this sand is given by Bueno et al.[8] All these parameters and the chemical reactions assumed in the system are summarized in Table 1.

Table 1. Morel Tableau for the TBT Reactive Transport Test-Case

	H^+	Cl^-	NO_3^-	Na^+	Im	TBT^+	≡S—OH	Ψ_S	Given log (K)
OH^-	−1								−14.0
Im H^+	1				1				7.0
Im TBT^+					1	1			3.91
TBTOH	−1					1			−6.25
TBTCl		1				1			0.6
$TBTNO_3$			1			1			0.62
$\equiv S—OH_2^+$	1						1	1	**4**
$\equiv S—O^-$	−1						1	−1	**−8**
≡S—OTBT	−1					1	1		**1.37**
$\equiv S—OHTBT^+$						1	1	1	**5.46**
≡S—ONa	−1			1			1		**−5.3**
Initial condition (M)	Fixed	0.0	0.1	0.1	10^{-3}	0.0	$\mathbf{10^{-5}}$		
Injection (M)	Fixed	$8.6\ 10^{-6}$	0.1	0.1	10^{-3}	$8.6\ 10^{-6}$			
Leaching (M)	Fixed	0.0	0.1	0.1	10^{-3}	0.0			

Given specific area[9] S = **0.200** $m^2 \cdot g^{-1}$. Bold parameters will be estimated.

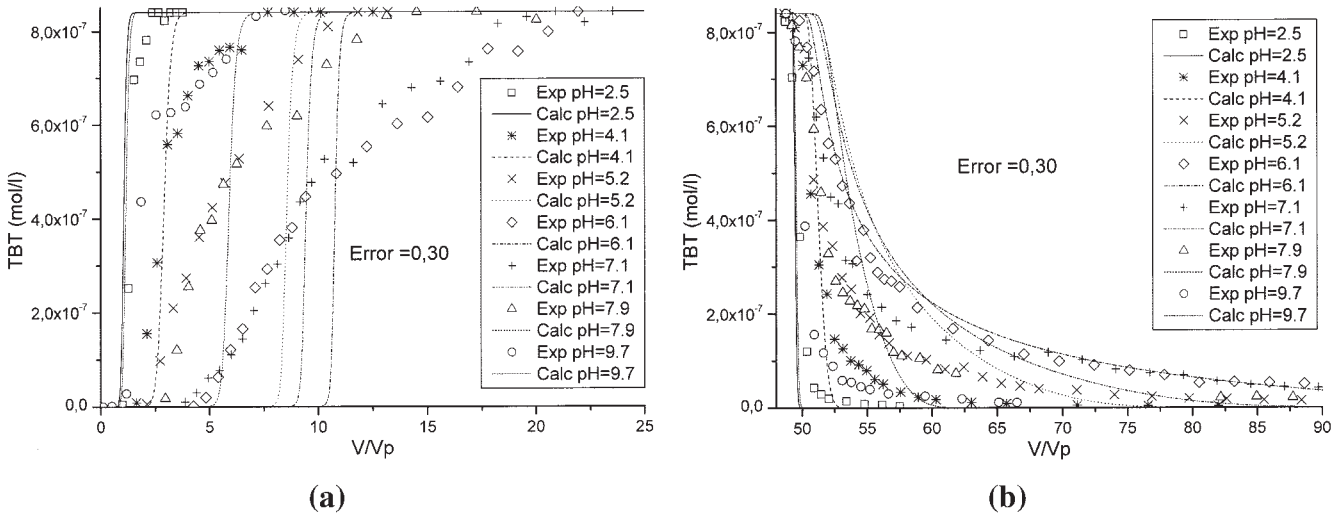

Figure 3. Experimental and initially calculated elution curves.

Initially calculated elution curves are obtained with *batch initial* parameters from Bueno et al.[8] Error function and parameters values are given in Table 2a and Figure 3a: injection of TBT into the column. Figure 3b leaching of TBT out of the column.

A measure of the point of zero charge (PZC) of the sand has been done.[9] The PZC of a surface is the pH where this surface is electrically neutral in pure water. Table 1 shows that in pure water, the quartz sand is supposed to form two species: $\equiv S\text{—}OH_2^+$ and $\equiv S\text{—}O^-$. The PZC is used here as additional information to select the acceptable sets of parameters by controlling the relation between the two equilibrium constants: $K_{\equiv S\text{—}OH_2^+}$ and $K \equiv S\text{—}O^-$. The experimental measure[9] gives

$$PZC = \frac{1}{2}\left[\log(K_{\equiv S-OH_2^+}) - \log(K_{\equiv S-O^-})\right] = 6 \pm 1 \quad (18)$$

The experimental column is 20 cm long, discretized in 20 cells. We use a Courant number equal to one, and a Pèclet number equal to five

$$CFL = \frac{U\Delta t}{\Delta x} = 1 \text{ and } Pe = \frac{U\Delta x}{D} = 5 \quad (19)$$

On the contrary of standard numerical methods (finite volume or finite element) which need a Peclet number less than two, the association of discontinuous finite element and mixed hybrid finite element used here has been successfully tested[20] for Peclet numbers less to 100.

Breakthrough curves obtained with these given parameters are compared with experimental ones in Figure 3. Elution part of the pH = 6.1 breakthrough curve is very well fitted to experimental data (Figure 3b). Indeed, we used parameters estimated at this pH. Unfortunately, the fitting of the elution curves to experimental data is not so good for other pHs, and not any injection curves is well described. The modelized system leads to sharp injection fronts instead of the experimental one which are a little diffusive (Figure 3a). In this work, we will answer the question: "Is the proposed set of parameters inaccurate, or is the set of reactions which does not describe accurately the phenomena?"

We will test the optimization procedure over this case in order to obtain one set of chemical parameter describing simultaneously these seven experiments. We set the same weights to all seven experiments, so that $\theta_{\text{Exp}} = 1$. There are a lot of experimental points at small concentrations (less than 10^{-7} mol $\cdot$ l^{-1}). Small concentrations are more represented, and then have a more important influence on the optimization procedure than higher concentrations. In order to give the same influence to all the concentration ranges we set the weight of experimental points as

$$\text{If } C_{Mes} > 10^{-7} \text{ mol} \cdot l^{-1} \text{ then } \theta_{Mes} = 1 \text{ else } \theta_{Mes} = 0.2 \quad (20)$$

The implementations presented previously to reduce CPU time allow us to run 2,000 realizations of these seven reactive transport problems in 26 h, on a COMPAQ Professional Workstation XP1000, with a physical memory of 1280.00 megabytes, and a 500 mHz EV6 processor.

Parameters estimation

The parameters estimation began from the *batch initial* set of parameters, with a restricted standard deviation (see Table 2a). We run $N_R = 2{,}000$ realizations, and $N_I = 100$. Through parameters estimation, the objective function is reduced from $F_N = 0.30$ for the *batch initial* parameters to $F_N = 0.261$ for the worst optimized set (Table 2b), and $F_N = 0.192$ for the best one (Table 2e). The set of parameters given in Table 2c is representative of the set usually found. As presented in the "expert analysis" section, we performed five searches from the same *batch initial* set.

We give in Table 2b the worst set found. Many indicators can help us to reject this set of parameters. The residual standard deviations are still large, more than 0.2 for equilibrium constants. Moreover, the *PZC* of the natural quartz sand is not accurately given by the estimated parameters

$$PZC = \frac{1}{2}\left[\log(K_{\equiv S-OH_2^+}) - \log(K_{\equiv S-O^-})\right] = \frac{1}{2}(6.17 + 8.04) = 7.10 \quad (21)$$

Table 2. Results of Parameter Estimation

F_N	Batch Parameters Figure 3 (a)		Worth Set Found Figure 4 (b)		Set Usually Found (c)		Best Set First Found (d)		2nd Optimization from (d) Figure 4 (e)		Longer Research N_R = 20 000 N_I = 1 000 (f)	
	0.30		0.261		0.204		0.201		0.1921		0.195	
	$\bar{P}$	σ	$\bar{P}$	σ	$\bar{P}$	σ	$\bar{P}$	σ	$\bar{P}$	σ	$\bar{P}$	σ
$\log(K_{\equiv S-OH_2^+})$	4	4	6.17	0.27	1.82	0.58	2.25	$3.8\ 10^{-2}$	2.90	$3.8\ 10^{-2}$	3	$2.1\ 10^{-2}$
$\log(K_{\equiv S-O^-})$	−8	4	−8.04	1.77	−9.35	0.31	−10.4	$2.3\ 10^{-2}$	−7.58	$3.8\ 10^{-2}$	−7.7	$4.3\ 10^{-2}$
$\log(K_{\equiv S-OTBT})$	1.37	4	0.99	0.43	1.46	$7.0\ 10^{-2}$	1.45	$5.4\ 10^{-3}$	1.16	$1.0\ 10^{-2}$	0.99	$9.2\ 10^{-3}$
$\log(K_{\equiv S-OHTBT^+})$	5.46	4	7.89	0.32	5.17	$7.3\ 10^{-2}$	5.30	$4.5\ 10^{-3}$	5.62	$4.0\ 10^{-3}$	5.7	$6.9\ 10^{-3}$
$\log(K_{\equiv S-ONa})$	−5.3	4	−7.03	0.45	−6.23	$4.1\ 10^{-2}$	−6.27	$3.9\ 10^{-3}$	−7.46	$3.2\ 10^{-1}$	−8.8	$8.9\ 10^{-2}$
[≡S—OH] (mol/l)	10^{-5}	10^{-5}	$5.78\ 10^{-6}$	$3.9\ 10^{-7}$	$6.55\ 10^{-6}$	$4.9\ 10^{-7}$	$6.44\ 10^{-6}$	$3.0\ 10^{-8}$	$6.92\ 10^{-6}$	$2.7\ 10^{-8}$	$6.50\ 10^{-6}$	$4.5\ 10^{-8}$
S (m^2/g)	0.200	0.11	0.231	$9.7\ 10^{-3}$	0.177	$1.4\ 10^{-3}$	0.206	$2.6\ 10^{-3}$	0.346	$5.6\ 10^{-3}$	0.203	$3.2\ 10^{-3}$

instead of having $PZC = 6 \pm 1$ (Eq. 18) from experimental data.

On the other hand, another set found (Table 2c) is given with a small residual standard deviation, less than 0.1 for sorption of TBT and Na^+ constants, but still a large one of acidity constants (more than 0.3). In this case, we can assume that acidity constants are not yet well estimated, whereas sorption ones are quite accurate. Even if acidity constants are still not well estimated, the *PZC* is accurately estimated

$$PZC = \frac{1}{2}\left[\log(K_{\equiv S-OH_2^+}) - \log(K_{\equiv S-O^-})\right] = \frac{1}{2}(1.82 + 9.35) = 5.58 \quad (22)$$

Finally, the best set found from the *batch initial* set with $N_R = 2{,}000$ (Table 2d), is given with a small residual standard deviation, less than $4\ 10^{-2}$ for all equilibrium constants. The objective function is $F_N = 0.201$. The *PZC* of the sand is accurately given by the estimated parameters

$$PZC = \frac{1}{2}\left[\log(K_{\equiv S-OH_2^+}) - \log(K_{\equiv S-O^-})\right] = \frac{1}{2}(2.25 + 10.4) = 6.45 \quad (23)$$

We can see that the total sorption site estimated concentration, and the specific areas are close to the proposed one, and are given with a very small residual standard deviation.

By running a long research, that is $N_R = 20{,}000$, and $N_I = 1{,}000$, a better optimization is obtained. The objective function is small $F_N = 0.195$, and the proposed set (see Table 2f) is close to the best set of parameter given in Table 2e. The standard deviations associated to this set of parameters are small. Because the calculation of $N_R = 20{,}000$ realizations is very long (20 days), it is much more efficient to run two or three times $N_R = 2{,}000$ realizations, especially because the proposed sets are equivalent.

Uniqueness of the fit

In order to know if the best set found after $N_R = 2{,}000$ realizations (Table 2d) is the better one, a second optimization is run. The initial set of parameters is now the set given in Table 2d. The initial standard deviations are reduced, and are half of those given initially in Table 2a. After this second optimization, a better set is obtained, given in Table 2f. This set is the best one with an error function of $F_N = 0.192$. No more improvement is obtained by running a third optimization from the set of parameters given in Table 2e. All the parameters are given with a small standard deviation indicating that the convergence has been efficient. The PZC proposed for this set of parameter is $PZC = 5.24$. This value is quite far away from the experimental value of $PZC = 6 \pm 1$, but is still acceptable. A qualitative analysis of the parameters sensitivity can be done by comparing the different sets of parameters proposed in Table 2c, d, e, and f. The equilibrium constants for $\mathbf{K}_{\equiv S-OH_2^+}$, $\mathbf{K}_{\equiv S-OTBT}$, and $\mathbf{K}_{\equiv S-OHTBT^+}$, the total concentration [≡S—OH], and the specific area *S* are always given with close values. On the other hand, equilibrium constants for $\mathbf{K}_{\equiv S-O^-}$ and $\mathbf{K}_{\equiv S-ONa}$ are very variable. These results are consistent with previous work.[21]

Table 3. Standard Deviation and Correlation Coefficients

	$\log(K_{\equiv S-OH_2^+})$	$\log(K_{\equiv S-O^-})$	$\log(K_{\equiv S-OTBT})$	$\log(K_{\equiv S-OHTBT^+})$	$\log(K_{\equiv S-ONa})$	[≡S—OH] (mol/l)	S (m^2/g)
$\log(K_{\equiv S-OH_2^+})$	**7,84E−03**						
$\log(K_{\equiv S-O^-})$	−6,46E−02	**4,61E−03**					
$\log(K_{\equiv S-OTBT})$	−8,85E−02	8,47E−01	**3,54E−03**				
$\log(K_{\equiv S-OHTBT^+})$	5,34E−01	−8,02E−03	−5,81E−02	**5,11E−03**			
$\log(K_{\equiv S-ONa})$	1,49E−01	−2,13E−02	1,29E−02	−4,16E−02	**5,78E−02**		
[≡S—OH] (mol/l)	−8,39E−02	−4,43E−01	−6,89E−01	−1,14E−01	1,54E−02	**6,08E−09**	
S (m^2/g)	−1,36E−01	−1,69E−01	−1,08E−01	−1,75E−02	−3,48E−02	1,61E−01	**1,64E−04**

Diagonal term (**bolt**) are the standard deviations for each parameter, nondiagonal one are correlations coefficients. We select 70 set of parameters with $F_N < 0.1923$.

This sensitivity analysis can be improved at low cost: from the optimization procedure, we get many set of parameters close to the optimal one. By selecting these which have an objective function sufficiently close to the best found (F_N = 0.1921), we obtain a representative set of accurate parameters. We select here the 70 set of parameters which have an objective function less than $F_N = 0.1923$. The standard deviation of these parameters and the correlation coefficients are given in Table 3. The standard deviation for each parameter is small. So we can assume that the best set of parameter is found with a sufficient precision. Because all the correlation coefficients are less than 0.9, the parameters are not correlated. This means that the hydrochemical system described in this work is not overparameterized. The standard deviation associated to $\mathbf{K}_{\equiv S-ONa}$ in Table 3 is more or less 10 times larger than the standard deviation for other equilibrium constants. This confirms previous results obtained by Tovo[21]: the equilibrium constant $\mathbf{K}_{\equiv S-ONa}$ does not have a significant influence on the objective function.

Breakthrough curves obtained using this best set of parameters is given in Figure 4. Comparing the results obtained after optimization (Figure 4) to these given from batch estimation (Figure 3) many improvement can be underlined. Elution curves at pH = 6.1 and 7.1 are much more similar according to experimental results. Retention of TBT at pH = 7.9 as been increased. A difference is now visible between elution at pH = 2.5, and elution at pH = 9.7 like for experimental curves. Injections curves have been changed a little bit. Injection at pH = 6.1 and 7.1 are much more similar, injection at pH = 5.2 is more delayed, and a difference is now visible between injection at pH = 2.5 and 9.7. Nevertheless, many problems are still present: even if injection curves seem to be slightly more diffusive, the calculated injection front is still compressive. Injection and leaching curves at pH = 7.9 are over delayed. Indeed, curves at pH = 7.9 are quite superposed with these obtained at pH = 6.1 and 7.1.

Conclusion

In this work, we develop a Monte-Carlo algorithm to optimize reactive transport parameters on multiconditional experiments. To use less computing time than a full random research, the mean and the standard deviation of the parameters are adapted during the optimization. This improvement allows us to use only 2,000 realizations of the reactive transport problem to find an accurate solution. Nevertheless, reducing computing time and the number of realizations introduces some hazard into the research procedure. It is also necessary to have some additional information, such as *PZC* value in our case, to validate the proposed set of parameters. In order to be sure of the proposed set of parameters, running many realizations is necessary too. As shown in Table 2, the results are not always

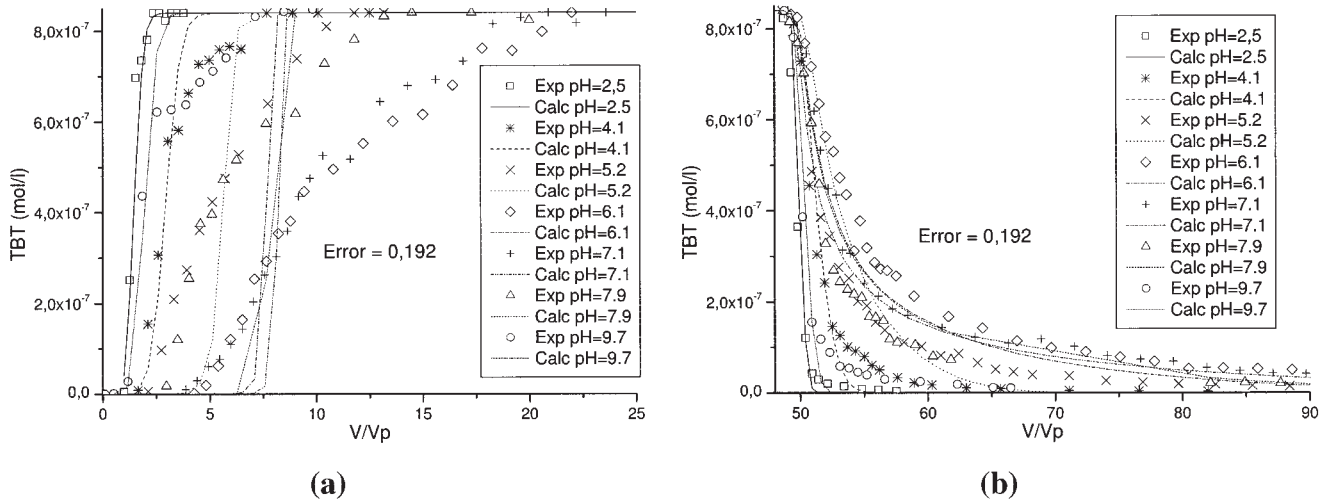

Figure 4. Experimental and optimized calculated elution curves.

Calculated elution curves are obtained after optimization with our algorithm. Estimated parameters obtained for N_R = 2,000 realizations as a second optimization from the best set found (Table 2d) at first optimization. F_N and **P** are given in Table 2e. Figure 4a: injection of TBT into the column. Figure 4b leaching of TBT out of the column.

the same. This is due to the reduction of the number of realizations, leading to a larger influence on the generated random numbers. Nevertheless, it is faster to run two or three times $N_R = 2{,}000$ realizations than to run one time $N_R = 10{,}000$ realizations, and leads to the same set of parameters. As shown by the correlation analysis, the set of parameters proposed by our algorithm is very accurate.

We have found many sets of parameters with an efficient convergence of the algorithm. Nevertheless, these sets of parameters are not the better one. This induces that the objective function has many local minima.

We have tried to find a set of parameters describing the seven injection-leaching experiments, assuming that the reactions governing the system are those given in Table 1. The best set of parameters found cannot describe accurately the experimental curves. This means that the proposed set of reactions does not represent the chemistry of TBT with the natural quartz sand. Bueno et al.[22] have shown, using experimental methods, that the sorption of TBT onto the natural quartz sand is better described by Langmuir-type isotherms with two sorption sites rather than by one. Nevertheless, a Langmuir isotherm can only describe the phenomena at one fixed pH, and does not take into account the electrostatic correction at the surface of the sand. The surface complexation model used in our work can describe the phenomena at various pHs, and takes into account the electrostatic correction. We can then answer the question posed previously, and we prove here that, even by describing more precisely the surface behavior during the sorption, one sorption site is not enough to represent accurately the sorption of TBT onto the natural quartz sand.

In this work, the natural quartz sand is described as an homogeneous surface with only one kind of sorption site: ≡S—OH. Analysis of this quartz sand[9,23] shows that the grain surface is composed of quartz, amorphous silica, ferric, and aluminum oxide and clay. According to our results, it seems that the macroscopic reactivity of a complex surface cannot be simplified to a unique sorption site if the pH is changing. This assumption has heavy consequences for the study of the sorption phenomena onto heterogeneous surface. Indeed, a macroscopic model, describing the sorption onto one site representing all the surface, will not be able to give an accurate overview of the phenomena, especially at various pHs. It is then necessary to produce more complex and complete sorption models, which take into account the heterogeneities of the surface. A further way of research will be to determine if all the heterogeneities have to be included into the sorption model, or if only the major ones are sufficient.

In order to increase the efficiency of the parameters estimation, more experimental information should be added. Only TBT elution curves have been used in this work. Sorption isotherms for batch experimentation can be added, or elution curves for other species. The effort done to reduce computing time must be continued, by increasing the efficiency of the chemical computation, and the reducing the number of time steps needed by transport model.

Acknowledgments

We thank Delphine Tovo (Ecole Nationale des Ingénieurs en Art Chimique et Technologique de Toulouse) for preliminary work during her engineer internship, and Ami Marxer for helpful comments. We thank Maïté Bueno for providing experimental data. M.A. has been supported by a grant from EGIDE.

Literature Cited

1. van der Lee J, De Windt L. Present state and future directions of modeling of geochemistry in hydrogeological systems. *J Contam Hydrol.* 2001;47:265–282.
2. Westall JC. FITEQL ver. 2.1. Corvallis, Department of Chemistry, Oregon State University; 1982.
3. Zhang T, Guay M. Adaptive parameter estimation for microbial growth kinetics. *AIChE J.* 2002;48:607–616.
4. Brassard P, Bodurtha P. A feasible set for chemical speciation problems. *Comps & Geosciences.* 2000;26:277–291.
5. Carrayrou J, Mosé R, Behra P. New efficient algorithm for solving thermodynamic chemistry. *AIChE J.* 2002;48:894–904.
6. Marshall SL. Generalized least-squares parameter estimation from multiequation implicit models. *AIChE J.* 2003;49:2577–2594.
7. Vikhansky A, Kraft M. A Monte Carlo methods for identification and sensitivity analysis of coagulation processes. *J Comput Phys.* 2004; 200:50–59.
8. Bueno M, Astruc A, Astruc M, Behra P. Dynamic sorptive behavior of tributyltin on quartz sand at low concentration levels: Effect of pH, flow rate, and monovalent cations. *Environ Sci Technol.* 1998;32: 3919–3925.
9. Bueno M. Etude dynamique des processus de sorption-désorption du tributylétain sur un milieu poreux d'origine naturelle. Université de Pau et des Pays de l'Adour, 1999. Ph.D. Thesis.
10. Carrayrou J. *Modélisation du transport de solutés réactifs en milieu poreux saturé.* Ph.D. thesis, Université Louis Pasteur Strasbourg I, 2001.
11. Sigg L, Behra P, Stumm W. *Chimie des milieux aquatiques.* Paris: DUNOD, 2000.
12. Morel FMM. *Principles of Aquatic Chemistry.* New York: Wiley Interscience, 1983.
13. Stumm W, Morgan JJ. Aquatic chemistry. Chemical equilibria and rates in natural waters. New York: Wiley-Interscience, 1996.
14. Dzombak DA, Morel FMM. Surface complexation modelling: Hydrous Ferric Oxide. New York; Wiley-Intersciences, 1990.
15. Stumm W. Chemistry of the solid-water interface. New York: Wiley-Interscience, 1992.
16. Yeh GT, Tripathi VS. A critical evaluation of recent developments in hydrogeochemical transport models of reactive multichemical components. *Water Resour Res.* 1989;25:93–108.
17. Steefel CI, MQuarrie KTB. Approaches to modelling of reactive transport in porous media. In: Lichtner PC, Steefel CI, Oelkers EH, eds. *Reactive Transport in Porous Media.* Washington: Mineralogical Society of America, 1996:82–129.
18. Carrayrou J, Mosé R, Behra P. Modelling reactive transport in porous media: iterative scheme and combination of discontinuous and mixed-hybrid finite elements. *C. R. Acad Sci., Ser. II Univers.* 2003;331:211–216.
19. Hardyanto W. Groundwater modelling taking into account probabilistic uncertainties. Freiberg on-line Geosciences; 2003; 10.
20. Siegel P, Mosé R, Jaffré J. Solution of the advection dispersion equation using a combination of discontinuous and mixed finite elements. *Int J Numer Methods Fluids.* 1997;24:595–613.
21. Tovo D. Prise en compte de l'incertitude dans l'estimation des paramètres du transport réactif par une méthode Monte-Carlo. ENSIACET. Toulouse: France, Rapport de stage ENSIACET; 2003.
22. Bueno M, Astruc A, Lambert J, Astruc M, Behra P. Effect of solid surface composition on the migration of tributyltin in groundwater. *Environ Sci Technol.* 2001;35:1411–1419.
23. Behra P, Lecarme-Theobald E, Bueno M, Ehrhardt JJ. Sorption of tributyltin onto a natural quartz sand. *J Colloid Interface Sci.* 2003; 263:4–12.

Manuscript received Oct. 8, 2004, revision received Oct. 5, 2005, and final revision received Feb. 6, 2006.